



HAL
open science

Theoretical mapping of interaction between alkali metal atoms adsorbed on graphene-like BC₃ monolayer

Kazem Zhour, Andrei V. Postnikov

► **To cite this version:**

Kazem Zhour, Andrei V. Postnikov. Theoretical mapping of interaction between alkali metal atoms adsorbed on graphene-like BC₃ monolayer. 2021. hal-03191539

HAL Id: hal-03191539

<https://hal.science/hal-03191539v1>

Preprint submitted on 15 Apr 2021

HAL is a multi-disciplinary open access archive for the deposit and dissemination of scientific research documents, whether they are published or not. The documents may come from teaching and research institutions in France or abroad, or from public or private research centers.

L'archive ouverte pluridisciplinaire **HAL**, est destinée au dépôt et à la diffusion de documents scientifiques de niveau recherche, publiés ou non, émanant des établissements d'enseignement et de recherche français ou étrangers, des laboratoires publics ou privés.

Theoretical mapping of interaction between potassium atoms adsorbed on boron carbide monolayer

Kazem Zhou^a and Andrei Postnikov^a

^a LCP-A2MC Université de Lorraine 1 Bd Arago, F-57078 Metz Cedex 3, France

Corresponding authors emails: kazem.zhour@gmail.com; andrei.postnikov@univ-lorraine.fr

Abstract

First-principles calculations using density functional theory and two methods in comparison, Quantum ESPRESSO and SIESTA, are done on large supercells which describe different placements of two adsorbed potassium atoms on the monolayer of boron carbide BC_3 . The energy of single K adsorption over the center of C_6 ring, of the C_4B_2 hexagon and over a boron atom are estimated to be 1.66, 1.63 and 1.58 eV, respectively; the comparison of these results with some available data is discussed. Exact theoretical estimations may be somehow sensitive to the lattice spacing practically used in the calculation. The interaction of two potassium atoms adsorbed at close enough distances (less than $\simeq 10$ Å) is negligible if the adsorption occurs at the opposite sides of the BC_3 layer, but creates a steep repulsive potential at distances less than $\simeq 8$ Å if the K atoms are adsorbed on the same side of the monolayer. Relaxation patterns resulting from the two K atoms being trapped at adjacent adsorption sites in the lattice are explained. The results suggest that the density of adsorbed K atoms on BC_3 can be interestingly high.

Keywords: semiconductor; monolayer; alkali metal; adsorption; diffusion.

1 Introduction

Boron carbide (BC_3) recently emerged [1] as an interesting two-dimensional (2D) material, in its structure and some properties close to graphene, with the difference that its single layer is semiconducting and not semi-metallic. Certain expectations are related with using this material functionalized with metals, for so different purposes as alkali metal storage in batteries [2], enhanced sensibilisation for gas sensing [3], and hydrogen storage [4]. These lines of research brought about recent works of first-principles simulation. Zhao *et al.* [5] probed different placements of Li, Na and K atoms over different sites of BC_3 , compared the corresponding adsorption energies, and traced the energy profiles across the barriers between adjacent adsorption sites. They used the VASP package on 3×3 supercells (of primitive cells with 2 formula units) and generalized gradient approximation for the exchange-correlation after the prescription of Perdew–Burke–Erznerhof (GGA-PBE) [6, 7]. Naqvi *et al.* [8] used the same calculation method (on a smaller, 2×2 supercell) to probe the docking of the same alkali metals and moreover of the alkaline earth metals, with subsequent adsorption of CH_4 , CO_2 and CO molecules at the metal sites. Bafekry *et al.* [9]

Table 1: Calculated properties of single-layer BC₃.

Method	Ref.	d_{C-C} (Å)	d_{C-B} (Å)	a (Å)	E_{gap} (eV)
SIESTA GGA	present work	1.428	1.564	5.183	0.67
QE GGA	present work	1.421	1.564	5.170	0.51
VASP GGA	[11]	1.422	1.565	5.174	0.62
VASP GGA	[5]	1.42	1.57	5.17	0.66
SIESTA GGA	[9]	1.422	1.562	5.17	0.7

explored different placements and estimated corresponding adsorption energies for a long list of adatoms and small molecules, in a series of calculations using OpenMX and SIESTA methods with GGA-PBE, for 2×2 supercell.

Whereas these studies permit to provide some consistent idea of how would the potassium atoms place themselves onto, and diffuse over, the BC₃ layer, we find it interesting to address a hitherto unexplored issue of interaction of K atoms at the surface. This may help to parametrise this interaction to adequately model the diffusion, and/or to estimate maximal density of K atoms to be placed on the surface, which may be helpful for the above discussed issues, i.e., battery electrodes or gas sensors. In view to probe this interaction, we considered supercells of larger size than in the mentioned previous studies, and decorated with two potassium atoms. Two calculation methods have been used in comparison; – SIESTA for principal large-size calculations and Quantum ESPRESSO for smaller-size benchmarks. The exchange-correlation potential used was GGA-PBE as in most of the other recent works; other calculation details can be found in Section 5. We start however with a short discussion of pristine BC₃ and the K adsorption on it in Section 2, checking ourselves against the previous results, and come to novel results concerning K–K interaction in Section 3. The conclusions are summarized in Sec. 4.

2 Pristine BC₃ and adsorption of K on it

Planar Boron carbide, described in Ref. [1], is characterized by a honeycomb planar lattice like that of graphene, in which one carbon atom out of four (equivalently, two atoms within a 2×2 graphene supercell) are substituted by boron. In principle, one can imagine different relative placements of B atoms on the honeycomb lattice, corresponding to para-, ortho- and meta-isomers (referred to as types A, B and C in Ref. [10]). However, the para-isomer is singled out by its more regular and symmetric arrangement in which every carbon atom has exactly one boron neighbour, and there are no B–B bonds. This isomer retains the hexagonal (super)structure, which makes a pattern of C₆ (perfect) hexagons with the C–C bond lengths $d_{C-C} \approx 1.4$ Å and C₄B₂ (distorted) hexagons around the perfect ones, with the C–B bond lengths $d_{C-B} \approx 1.6$ Å. The lattice parameter of this hexagonal unit cell which hosts two formula units is $a = \sqrt{3}(d_{C-C} + d_{C-B})$. Differently from perfect infinite graphene which has a zero gap, BC₃ has the band gap of 0.65 eV (in a single sheet). A summary of previous data concerning pristine BC₃, along with our present results, is given in Table 1.

The works aimed at the study of K adsorption on BC₃ from first principles are not numerous. Understandably, the possible adsorption sites probed in previous works (notably

Zhao *et al.*[5]) are over the center of one or another hexagon, over the C–C or C–B bonds, or over the one or the other atom species. Zhao *et al.* argued (with respect to Li, Na and K on BC₃, which we confirm in our study of K), that only three of these sites, over the both hexagons and atop a boron atom, emerge as local energy minima for adsorption.

There seems to be a consensus among the calculations done that the hollow site over the center of the C₆ hexagon, referred to as HC in the following, is the preferential one, closely followed by the hollow site over the center of the C₄B₂ hexagon, referred to as HB. With respect to the value of the adsorption energy, however, there seems to be a controversy we show in Table 2. We performed this calculation using sufficiently large supercell (in terms of B₂C₆ unit cells) per adsorption atom and inspected several possible sources of controversy. Without much details given in the papers cited, good “suspects” could be the basis set superposition error (BSSE, Ref. [12]) (potentially dangerous in methods with atom-centered basis functions, e.g., Ref. [9]), and the neglect of the magnetic state for an isolated potassium atom, both factors tending to overestimate the adsorption energy. Our result shown in Table 2 is obtained from comparing the energies of two sufficiently thick supercells of identical size, possessing the same 73 atoms: the relaxed system upon K adsorption, and the pristine BC₃ layer with the K atom removed away from the layer at a distance that would preclude the overlap of their basis functions. This does not fully removes the BSSE (that could have been done by introducing ghost atoms), but substantially cancels systematic errors.

A smooth variation of the total energy and magnetic moment on approaching the K atom to the BC₃ sheet (without performing any structure relaxation and only converging the electronic structure) is depicted in Fig. 1. For the record, the lattice parameter in these trial calculations done with SIESTA was fixed at $a = 5.143 \text{ \AA}$, somehow smaller than the value we preferred to use in our supercell calculations. However, the comparison with our “approved” estimations for the K adsorption energy (obtained in more accurate and fully relaxed calculations, to be discussed below) with the present “scan” helps to estimate the stability of results against small variations of the lattice parameter and to give a certain confidence in the values reported. The depth of the total energy profile gives a fair estimate of the adsorption energy. The magnetic moment exhibits instability throughout the range of distances 3 to 7 \AA , as the 4s state of potassium, which carries an unpaired spin in a free atom, starts to interact with the wavefunctions of the CB₃ layer. Upon adsorption and after atomic and electronic relaxation, the magnetic moment is fully dissolved (differently from the situation with graphene, on which the adsorbed K atom retains its magnetic moment).¹

The results obtained with the fixed lattice parameter of the supercell as optimized in QE calculation and following the unconstrained relaxation, comparing the total energies from “adsorbed K” and “distant K” situations within the same calculation setup, are shown in Table 2. For comparison, the calculation done with summing up the energies of BC₃-only supercell and “single-K-only” supercell yields the adsorption energies of $\simeq 2.1 \text{ eV}$.

Independently, we calculated the adsorption energy at HC and HB sites by the QE method, also for the $3 \times 3 \times 1$ supercell, referring in this case to the total energy differences of the kind (Supercell with adsorbed K) – [(Supercell without K) + (Single K atom in the box)], which approach is less problematic when using a planewave-basis code not prone to

¹The asymptotic value of the magnetic moment corresponding to large distances in Fig. 1 does not reach $1 \mu_B$ – probably due to a purely technical drawback that very fine \mathbf{k} and energy mesh is needed to cope with very narrow K4s energy levels.

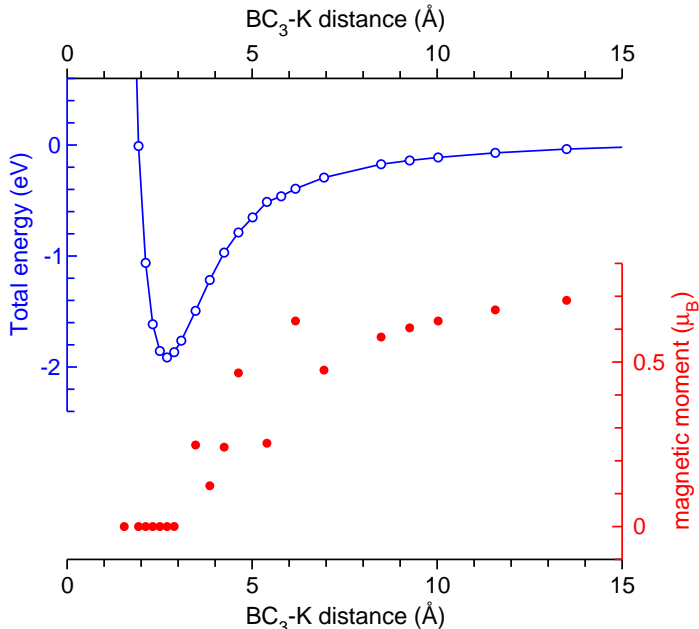


Figure 1: Total energy (upper panel, blue line) and magnetic moment (lower panel, red line) profiles as functions of the height of the K atom over the BC_3 layer. Calculations are done with lattice constant fixed at $a = 5.143 \text{ \AA}$ without structure relaxation.

Table 2: Calculated parameters of K adsorption over the C_6 hexagon on BC_3 . E_a : adsorption energy (corresponding to energy gain on adsorption, in all cases); h : the height of the adsorbed atom over the BC_3 plane. See text for detail.

Method	Ref.	Supercell	E_a (eV)	h (\AA)
SIESTA GGA	[9]	$2 \times 2 \times 1$	0.82^a	2.569
VASP GGA	[8]	$2 \times 2 \times 1$	4.72	2.53
VASP GGA	[5]	$3 \times 3 \times 1$	1.75	2.57
SIESTA GGA	present work	$3 \times 3 \times 1^*$	$1.66^a, 1.63^b, 1.58^c$	$2.68^a, 2.67^b$
QE GGA	present work	$3 \times 3 \times 1^*$	$2.31^a, 2.25^b$	$2.63^a, 2.62^b$

* $a=5.17 \text{ \AA}$ fixed; a HC position; b HB position; c over C-B bond.

BSSE. The results are 2.31 eV for the HC site and 2.25 eV for the HB site. Notwithstanding a slight variance with the SIESTA results, we can anyway conclude that the adsorption energy of K on BC_3 is likely to be of the order of 2 eV, close to the result by Zhao *et al.*, rather than the other two reported values, apparently strongly under- or correspondingly overestimated. The magnitude of the adsorption energy being thus settled, the differences between the adsorption at different sites seem mild and less controversial. In comparison with the adsorption energies of 1.66 eV at HC position, we arrive at 1.63 eV at HB and 1.58 eV in AB (on top of the B atom). This span is in good agreement with the energy profiles (“diffusion paths”) shown in Fig. 5(d) of Ref. [5], according to which the HB position is $\simeq 0.05$ eV higher than HC, and the barrier between two adjacent hexagons is about 0.12 eV

high. Our QE estimation of the energy difference between HC and HB sites confirms the energy difference between HC and HB to be $\simeq 0.05$ eV. The effect of disperse interactions, included in Ref. [5] within the simplified Grimme scheme [13] but neglected in our work, may be in part responsible for the remaining numerical difference.

Apart from Ref. [5], we are not aware of other works dealing with the “diffusion profiles” of K on BC_3 . Our simulation confirms a peculiar property of potassium to combine appreciable adsorption energy (hence well sticking to the surface of BC_3) with very flat energy landscape (hence presumably good mobility over this surface). In the next section, we come to the analysis of interaction between K atoms.

3 Interaction of K atoms adsorbed on BC_3

3.1 Spatial map of K–K interaction energies on the BC_3 surface

In order to gain a substantial and reliable information concerning the interaction between K atoms adsorbed on BC_3 , we staged a series of simulations on large supercells containing two potassium atoms. One of them, the “reference atom”, was adsorbed at a (lowest-energy) HC position over the center of a C_6 ring, and the other, “trial” atom – at different local-minima positions at different distances from the reference atom. Within the 5×5 supercell (200 atoms), all non-equivalent adsorption positions have been explored within the “irreducible wedge” (shown in inset of Fig. 2) closest to a given HC site. This amounted to four HC positions, 9 HB positions (over the center of C_4B_2 hexagons) and 7 AB positions (atop of a boron atom), hence the positions confirmed (see previous Section) to correspond to stable (local energy minima) adsorption sites. Moreover, the configurations in which the second (trial) atom was adsorbed at the opposite side of the CB_3 monolayer has been tested – on all the HC, HB and AB sites, mentioned above, plus directly at the reference site, in a mirror position from the reference atom. In all cases, an unconstrained relaxation has been performed (fixing however the supercell parameters), which yielded the total energy and the equilibrium geometry.

For K–K distances starting from $\sim 7 \text{Å}$ onwards, the relaxation patterns are barely visible: the adsorbed atoms reside in their nominal positions, so that only tiny modifications of interatomic distances come about. The CB_3 layer in all cases looks extremely rigid and planar, without a marked tendency towards bending or warping. At shorter distances, the repulsion between the adsorbed atoms pushes them out of symmetry positions; the examples of this will be discussed below. In fact, the stabilisation of the trial atom in the nearest HB or AB position to the reference atom becomes impossible, because the atoms drift away from such configuration. This refers to the atoms adsorbed at the same side of the CB_3 plane. The atoms adsorbed “across the plane” remain practically insensitive to the closeness of the reference atom, exhibiting no perturbations in their relaxation pattern, and the energies which are largely independent on the in-plane distance to the reference atom.

The “interaction energies” plotted in Fig. 2 are the free energies from the calculations, expressed relative to the lowest one over all configurations corresponding to the given placement (i.e., either above, or below the BC_3 layer) of the trial atom. In fact, this lowest energy stems from the most distant HC configuration, which effectively sets the “infinity” limit for the two K atoms being in maximally distant lowest-energy (i.e., HC) positions.

We note that these “infinity limit” energies are not exactly equal for the trial atom being on the same side of the BC_3 plane as the reference atom, or on the opposite side. In fact, the second energy is lower by 0.05 eV. This disparity (which would disappear be the atoms at really sufficiently far distance) can be considered as a measure of the effect of our limited supercell size.

Choosing such “distant K–K” limit of two adsorbed atoms as the reference level leaves the *adsorption energy* at a HC site out of our grasp; however, this issue has been separately addressed in the previous Section. On the contrary, the *differences* between adsorption energies at HC, HB and AB sites, or otherwise the barrier heights, are easily readable from Fig. 2, and are instructive to discuss.

We note first that for “inverted” adsorption of a trial atom, the energy of its interaction

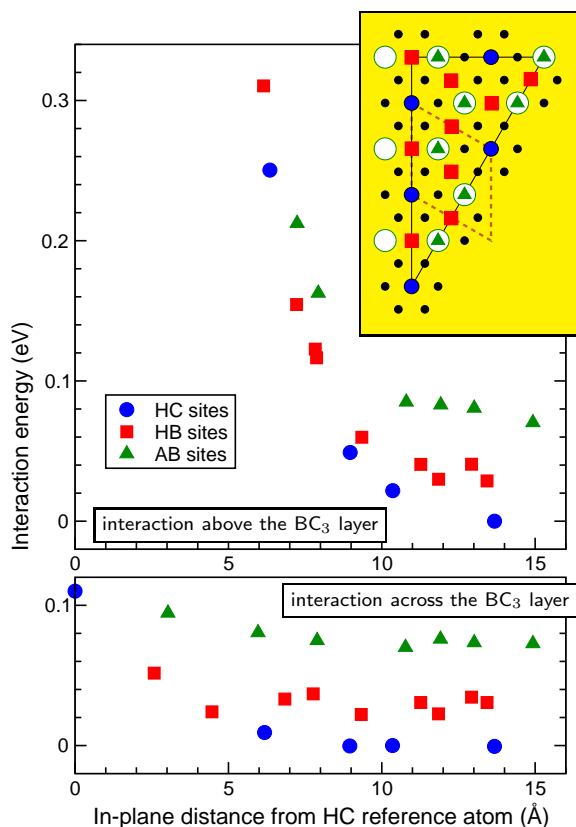


Figure 2: Map of interaction energies between K atoms adsorbed at different sites of the BC_3 lattice and the reference K atom in the HC position (the bottom blue point in the inset). HC positions (over C_6 hexagons), HB positions (over C_4B_2 hexagons) and AB positions (over B atoms) are indicated by different symbols. The upper panel maps the interactions between K atoms adsorbed at the same side of the CB_3 plane, the bottom panel – between atoms adsorbed at the opposite sides, in both cases – as function of the in-plane distances between the adsorption sites. The inset shows the projections of (ideal) adsorption sites of the three types onto the “irreducible part” (drawn as a triangle) of a 5×5 supercell. Positions included in the mapping are marked by symbols, as in the main plot. A primitive cell of BC_3 is outlined by a dashed contour.

with the reference one is practically independent on interatomic distance, and follows the universal trend that HB positions are, on the average, higher in energy by $\simeq 0.03$ eV than the HC ones, whereas the AB positions are higher than the HC by $\simeq 0.08$ eV. This simply passes the information about barrier heights (differences between adsorption energies at different sites), which was already addressed in the previous Section. However, here it appears not as a “random” number but as a “statistically credible” result. We can again refer to the similarity of the present estimation of barrier heights with those given by Zhao *et al.* [5], notably in Fig. 5(d) of this publication.

The bottom panel of Fig. 2 suggests that the K atoms “do not see each other” across the BC_3 plane till the K–K distance becomes really short, within the closest adsorption sites. Still, this does not bring about neither an “asymmetric” relaxation nor noticeable augmentation of the z -coordinate; the adsorbed atoms remain well centered at their respective sites. The “double occupation” of a HC adsorption site from both sides of the BC_3 plane, whereby the two K atoms remain stable at a distance 5.4 \AA (hence at a regular height above the layer) is by far not so energetically unfavourable as it could have been *a priori* anticipated; it costs only 0.1 eV to bring a K atom from any distant HC site onto the reference site.

The established hierarchy of barrier heights, revealed via interaction energies being independent on the K–K distance, is also valid for adsorptions at the same side of the BC_3 plane (see upper panel of Fig. 2), provided the K atoms are placed not closer than $\simeq 10 \text{ \AA}$. At shorter distances, the energy barrier rapidly increases, forming a nearly rigid core of the radius of $\simeq 6.1 \text{ \AA}$, irrespectively of the adsorption site concerned.

3.2 Unusual relaxation patterns of closely placed adsorbed atoms

The placement of trial atoms at adsorption sites close (within $\simeq 8 \text{ \AA}$) of the reference atom resulted in a noticeable repulsion of both atoms in their relaxed configurations, as shown in Fig. 3. The reference atom displaces in its “nest” over the C_6 ring without however leaving the latter, whereas the trial atom could have been pushed from its initial “on top of B” position onto that above the C–B bond; see the case AB in Fig. 3. It was not possible

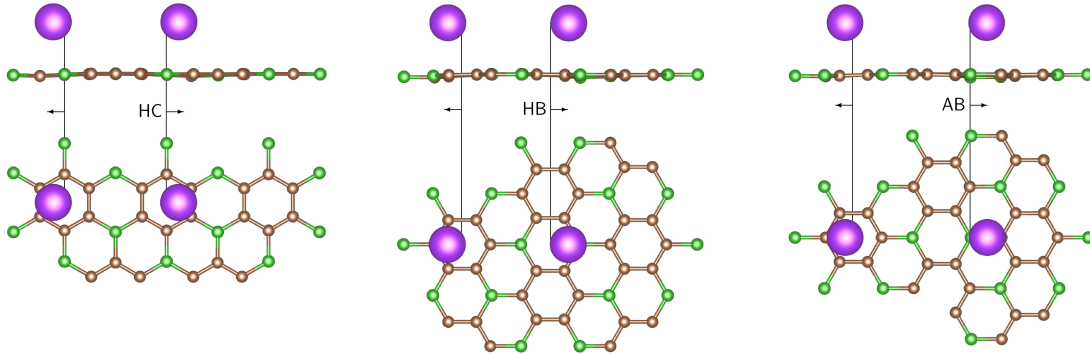


Figure 3: Relaxed structures (in side and top views) of trial K atoms initially placed at HC, HB and AB positions close to the reference K atom (that in the left of each plot). The arrows indicate the movement of the both K atoms apart.

the interacting atoms were pushed apart into “second-neighbors” configurations, shown in Fig. 3. This strengthens an idea of “hard core” repulsion potential which effectively prevents the potassium atoms to come closer than about 6 Å. This minimal distance corresponds to both atoms residing over the second-neighbour C₆–C₆ or C₆–C₄B₂ hexagons, slightly pushed apart from the respective centers, as shown in Fig. 3. We note that the *z*-coordinates of potassium atoms are not much affected by their relaxation “situation”; also the warping of the BC₃ layer, although noticeable around such “strong” relaxations, remains small and difficult to make sense of.

4 Conclusion

Summarizing, we found that potassium atoms adsorbed over the BC₃ monolayer interact strongly repulsively at distances smaller than $\simeq 10$ Å, and otherwise remain relatively insensitive to the mutual presence, feeling the “usual” landscape of potential barriers of $\lesssim 0.1$ eV in their movement over the BC₃ plane. A combination of relatively high adsorption energy ($\simeq 1.7$ eV) with respectively low barriers, known already from early works, presumed already an interesting interplay of sticking and mobility. Now we conclude that even relatively high concentration of adsorbed K atoms might not prevent them from acting as a highly mobile “gas” on the BC₃ surface. This may open perspectives for further more realistic simulations and interesting applications.

5 Calculation methods and technical details

We used two first-principles DFT methods in comparison, the plane-wave pseudopotential Quantum ESPRESSO (QE) [14, 15] and numerical orbitals pseudopotential SIESTA [16, 17]. Exchange-correlation was treated within the GGA, using the PBE parametrisation [6, 7]. SIESTA is generally expected to be more efficient than planewave methods in treating large open low-coordinated systems, but, at the same time, potentially sensitive to the “quality” of fixed basis functions adopted. After some tests, we found it sufficient to use double-zeta basis functions for all atoms, including notably $3p$ as a valence state for potassium. The pseudopotentials used were norm-conserving, generated according to the Trouiller – Martins scheme [18] for the following free-atom configurations (the cutoff radii in Bohr being indicated in parentheses for each *l*-channel) : K $4s^1(3.14) 3p^6(1.83) 3d^0(3.14) 4f^0(2.54)$, B $2s^2(1.74) 2p^1(1.74) 3d^0(1.74) 4f^0(1.74)$, C $2s^2(1.54) 2p^2(1.54) 3d^0(1.54) 4f^0(1.54)$. The PAO.EnergyShift parameter in SIESTA was set to 0.015 Ry, that resulted in the maximal extension of basis functions of 5 Å.

In QE calculations, the kinetic energy and the charge density cutoffs were set to 50 Ry and 400 Ry, respectively. The convergence threshold for self-consistency in energy was set to 10^{-7} Ry. A $8 \times 8 \times 1$ undisplaced **k** mesh was employed in electronic structure calculations for pristine BC₃, with appropriate reduction in larger supercells. Ultrasoft pseudopotentials have been used.

Supporting Information

which includes detailed tables with adsorption geometry and energies for all the adsorption sites probed is available from the Wiley Online Library or from the author.

Acknowledgements

The authors acknowledge the support of the Erasmus mobility program which made possible for K.Zh. his research stay in Metz, and the mesocenter of calculation EXPLOR at the Université de Lorraine (project 2019CPMXX0918) for access to computation facilities.

References

- [1] H. Tanaka, Y. Kawamata, H. Simizu, T. Fujita, H. Yanagisawa, S. Otani, C. Oshima, *Solid State Communications* **2005**, *136*, 1 22.
- [2] Y. Qie, J. Liu, S. Wang, S. Gong, Q. Sun, *Carbon* **2018**, *129* 38.
- [3] S. Mehdi Aghae, M. M. Monshi, I. Torres, S. M. J. Zeidi, I. Calizo, *Applied Surface Science* **2018**, *427* 326.
- [4] S. Aydin, M. Şimşek, *International Journal of Hydrogen Energy* **2019**, *44*, 14 7354.
- [5] L. Zhao, Y. Li, G. Zhou, S. Lei, J. Tan, L. Lin, J. Wang, *Chinese Chemical Letters* **2020**.
- [6] J. P. Perdew, K. Burke, M. Ernzerhof, *Phys. Rev. Lett.* **1996**, *77*, 18 3865.
- [7] J. P. Perdew, K. Burke, M. Ernzerhof, *Phys. Rev. Lett.* **1997**, *78*, 7 1396.
- [8] S. R. Naqvi, T. Hussain, S. R. Gollu, W. Luo, R. Ahuja, *Applied Surface Science* **2020**, *512* 145637.
- [9] A. Bafekry, S. Farjami Shayesteh, M. Ghergherehchi, F. M. Peeters, *Journal of Applied Physics* **2019**, *126*, 14 144304.
- [10] I. V. Zaporotskova, S. V. Boroznin, *Modern Electronic Materials* **2017**, *3*, 2 91.
- [11] B. Mortazavi, M. Shahrokhi, M. Raeisi, X. Zhuang, L. F. C. Pereira, T. Rabczuk, *Carbon* **2019**, *149* 733.
- [12] S. F. Boys, F. Bernardi, *Molecular Physics* **1970**, *19* 553.
- [13] S. Grimme, *Journal of Computational Chemistry* **2006**, *27*, 15 1787.
- [14] P. Giannozzi, S. Baroni, N. Bonini, M. Calandra, R. Car, C. Cavazzoni, D. Ceresoli, G. L. Chiarotti, M. Cococcioni, I. Dabo, A. Dal Corso, S. de Gironcoli, S. Fabris, G. Fratesi, R. Gebauer, U. Gerstmann, C. Gougoussis, A. Kokalj, M. Lazzeri, L. Martin-Samos, N. Marzari, F. Mauri, R. Mazzarello, S. Paolini, A. Pasquarello, L. Paulatto, C. Sbraccia, S. Scandolo, G. Sclauzero, A. P. Seitsonen, A. Smogunov, P. Umari, R. M. Wentzcovitch, *Journal of Physics: Condensed Matter* **2009**, *21*, 39 395502.
- [15] P. Giannozzi, O. Andreussi, T. Brumme, O. Bunau, M. Buongiorno Nardelli, M. Calandra, R. Car, C. Cavazzoni, D. Ceresoli, M. Cococcioni, N. Colonna, I. Carnimeo, A. Dal Corso, S. de Gironcoli, P. Delugas, R. A. DiStasio Jr, A. Ferretti, A. Floris, G. Fratesi, G. Fugallo, R. Gebauer, U. Gerstmann, F. Giustino, T. Gorni, J. Jia, M. Kawamura, H.-Y. Ko, A. Kokalj, E. Küçükbenli, M. Lazzeri, M. Marsili, N. Marzari, F. Mauri,

- N. L. Nguyen, H.-V. Nguyen, A. Otero-de-la Roza, L. Paulatto, S. Poncé, D. Rocca, R. Sabatini, B. Santra, M. Schlipf, A. P. Seitsonen, A. Smogunov, I. Timrov, T. Thonhauser, P. Umari, N. Vast, X. Wu, S. Baroni, *Journal of Physics: Condensed Matter* **2017**, *29*, 46 465901.
- [16] J. M. Soler, E. Artacho, J. D. Gale, A. García, J. Junquera, P. Ordejón, D. Sánchez-Portal, *Journal of Physics: Condensed Matter* **2002**, *14*, 11 2745.
- [17] A. García, N. Papior, A. Akhtar, E. Artacho, V. Blum, E. Bosoni, P. Brandimarte, M. Brandbyge, J. I. Cerdá, F. Corsetti, R. Cuadrado, V. Dikan, J. Ferrer, J. Gale, P. García-Fernández, V. M. García-Suárez, S. Garcí, G. Huhs, S. Illera, R. Korytár, P. Koval, I. Lebedeva, L. Lin, P. López-Tarifa, S. G. Mayo, S. Mohr, P. Ordejón, A. Postnikov, Y. Pouillon, M. Pruneda, R. Robles, D. Sánchez-Portal, J. M. Soler, R. Ullah, V. W.-z. Yu, J. Junquera, *The Journal of Chemical Physics* **2020**, *152*, 20 204108.
- [18] N. Troullier, J. L. Martins, *Phys. Rev. B* **1991**, *43* 1993.